doi:10.1093/brain/aws013 Brain 2012: 135; 807–818 | 807

BRAIN
A JOURNAL OF NEUROLOGY

Acetylated tau, a novel pathological signature in Alzheimer's disease and other tauopathies

David J. Irwin,[1,2] Todd J. Cohen,[1] Murray Grossman,[2] Steven E. Arnold,[1,2,3] Sharon X. Xie,[4] Virginia M.-Y. Lee[1] and John Q. Trojanowski[1]

1 Centre for Neurodegenerative Disease Research, Department of Pathology and Laboratory Medicine, Alzheimer's Disease Core Centre, Institute on Ageing, University of Pennsylvania School of Medicine, Philadelphia, PA 19104-6021, USA
2 Department of Neurology, University of Pennsylvania School of Medicine, Philadelphia, PA 19104-6021, USA
3 Brain-Behaviour Laboratory, Department of Psychiatry, University of Pennsylvania School of Medicine, Philadelphia, PA 19104-6021, USA
4 Department of Biostatistics and Epidemiology, University of Pennsylvania School of Medicine, Philadelphia, PA 19104-6021, USA

Correspondence to: John Q. Trojanowski, MD,
Centre for Neurodegenerative Disease Research and Institute on Ageing,
Department of Pathology and Laboratory Medicine,
University of Pennsylvania School of Medicine,
HUP, Maloney 3rd Floor,
36th and Spruce Streets,
Philadelphia, PA 19104-4283, USA
E-mail: trojanow@mail.med.upenn.edu

The microtubule-binding protein, tau, is the major component of neurofibrillary inclusions characteristic of Alzheimer's disease and related neurodegenerative tauopathies. When tau fibrillizes, it undergoes abnormal post-translational modifications resulting in decreased solubility and altered microtubule-stabilizing properties. Recently, we reported that the abnormal acetylation of tau at lysine residue 280 is a novel, pathological post-translational modification. Here, we performed detailed immunohistochemistry to further examine acetylated-tau expression in Alzheimer's disease and other major tauopathies. Immunohistochemistry using a polyclonal antibody specific for acetylated-tau at lysine 280 was conducted on 30 post-mortem central nervous system regions from patients with Alzheimer's disease (10 patients), corticobasal degeneration (5 patients), and progressive supranuclear palsy (5 patients). Acetylated-tau pathology was compared with the sequential emergence of other tau modifications in the Alzheimer's disease hippocampus using monoclonal antibodies to multiple well-characterized tau epitopes. All cases studied showed significant acetylated-tau pathology in a distribution pattern similar to hyperphosphorylated-tau. Acetylated-tau pathology was largely in intracellular, thioflavin-S-positive tau inclusions in Alzheimer's disease, and also thioflavin-S-negative pathology in corticobasal degeneration and progressive supranuclear palsy. Acetylated-tau was present throughout all stages of Alzheimer's disease pathology, but was more prominently associated with pathological tau epitopes in moderate to severe-stage cases. These temporal and morphological immunohistochemical features suggest acetylation of tau at this epitope is preceded by early modifications, including phosphorylation, and followed by later truncation events and cell death in Alzheimer's disease. Acetylation of tau at lysine 280 is a pathological modification that may contribute to tau-mediated neurodegeneration by both augmenting losses of normal tau properties (reduced solubility and microtubule assembly) as well as toxic gains of function (increased tau fibrillization). Thus, inhibiting tau acetylation could be a disease-modifying target for drug discovery target in tauopathies.

Keywords: Alzheimer's disease; tauopathy; acetylation; post-translational modification; tau

Received September 10, 2011. Revised December 1, 2011. Accepted December 2, 2011

Introduction

Tau, an intracellular protein involved in promoting microtubule stability and neuronal survival, is the major component of inclusions seen in Alzheimer's disease and other related neurodegenerative tauopathies (Lee *et al*., 2001). Under normal conditions, tau is a highly soluble protein lacking significant secondary structure (Schweers *et al*., 1994). However, it undergoes several post-translational modifications resulting in fibrillization into straight- and paired-helical filaments. Paired-helical filaments coalesce to form neurofibrillary tangles, the hallmark lesions in Alzheimer's disease. Significantly, the burden of tau pathology correlates well with clinical symptoms of dementia in Alzheimer's disease (Jack *et al*., 2010).

Biochemical and immunohistochemical experiments using monoclonal antibodies raised to epitopes from Alzheimer's disease brain homogenates (Wolozin *et al*., 1986) and purified paired-helical filaments (Novak *et al*., 1989) have determined that tau undergoes abnormal folding (Carmel *et al*., 1996; Jicha *et al*., 1997a), hyperphosphorylation at multiple serine and threonine residues and C-terminal truncation (Novak *et al*., 1993) during neurofibrillary tangle-induced neurodegeneration in Alzheimer's disease (Buee *et al*., 2000). Indeed, tau hyperphosphorylation *in vitro* inhibits tau microtubule-binding activity (Biernat *et al*., 1993; Bramblett *et al*., 1993) and tau isolated from Alzheimer's disease autopsy tissue is highly phosphorylated (Lee *et al*., 1991). However, the direct role of hyperphosphorylation in tau aggregation is less clear, since *in vitro* experiments suggest this augments tau aggregation (Liu *et al*., 2007; Rankin *et al*., 2007), while phosphorylation at some tau residues appears to inhibit paired-helical filament formation (Schneider *et al*., 1999). Moreover, many tau phosphorylation sites also are found in normal control (Matsuo *et al*., 1994) and foetal brain tissue (Bramblett *et al*., 1993), although overall these sites are more extensively phosphorylated in Alzheimer's disease compared with normal brain (Mercken *et al*., 1992; Matsuo *et al*., 1994; Hoffmann *et al*., 1997). Since hyperphosphorylated foetal tau does not form inclusions, and non-phosphorylated tau can aggregate and fibrillize *in vitro*, hyperphosphorylation alone cannot fully explain the formation of tau pathology in Alzheimer's disease (Buee *et al*., 2000; Lee *et al*., 2001). Therefore, additional modifications of tau may influence its solubility and function as well as contribute to the pathobiology of tau inclusion formation.

Recently, tau was demonstrated to be modified by lysine acetylation (Min *et al*., 2010; Cohen *et al*., 2011) and we showed that tau undergoes acetylation at lysine 280 (K280) in the second microtubule-binding repeat of tau isoforms with four microtubule-binding repeats (i.e. 4R-tau) (Cohen *et al*., 2011). Acetylation at K280 inhibited tau-dependent microtubule assembly and increased tau fibrillization *in vitro*, while an acetylated K280 tau-specific polyclonal antibody labelled tau inclusions in Alzheimer's disease and other 4R-tau tauopathies, as well as in tau transgenic mouse models of tauopathies (Cohen *et al*., 2011). In addition, acetylated K280 was not detectable in normal control human and mouse brain, suggesting that acetylation of tau at this residue is a pathogenic modification in neurofibrillary tangle formation.

To determine the significance of tau acetylation, we performed an extensive immunohistochemical analysis to define the regional distribution of acetylated K280 immunoreactive tau pathology in Alzheimer's disease and two tauopathies with prominent 4R-tau pathology, i.e. corticobasal degeneration and progressive supranuclear palsy. We also characterized the emergence of acetylated K280-immunoreactive tangles in relation to those neurofibrillary changes induced by misfolded tau and hyperphosphorylated tau in the Alzheimer's disease hippocampus to assess the temporal course of acetylated K280-immunoreactive tau pathology in tangle formation.

Materials and methods

Patient selection

Cases were selected from the Centre for Neurodegenerative Disease Research (CNDR) Brain Bank at The University of Pennsylvania following formal neuropathological diagnosis as previously described (Forman *et al*., 2006) and in accordance with local institutional review board guidelines. Pathological diagnosis, demographic information and post-mortem interval (Table 1) were obtained from the CNDR integrated neurodegenerative disease database (Xie *et al*., 2011). We sampled 30 regions of the CNS in 10 cases of Alzheimer's disease, five cases of corticobasal degeneration and five cases of progressive supranuclear palsy to examine regional distributions of acetylated K280-immunoreactive tau pathology. Further detailed morphological assessment was performed in hippocampal sections in Alzheimer's disease cases over a range of severity stages (Braak and Braak, 1991) including 10 severe (Braak V and VI) and five moderate (Braak III and IV) stage Alzheimer's disease cases, as well as five mild (Braak I and II) stage controls.

Immunohistochemistry

Fresh tissue obtained at autopsy was fixed in 70% ethanol and 150 mmol sodium chloride, paraffin-embedded and 6-μm sections were cut and stained for immunohistochemistry as previously described (Forman *et al*., 2006; Cohen *et al*., 2011) utilizing an avidin–biotin complex detection system (VECTASTAIN® ABC kit; Vector Laboratories) with 3,3′-diaminobenzidine as the chromogen. Slides were pretreated for antigen retrieval with 88% formic acid or boiling in a pressure cooker using a citric acid unmasking solution (Vector Laboratories), with the exception of single-label experiments using monoclonal antibodies Alz50 and paired-helical filament-1.

The affinity-purified polyclonal antibody specific for acetylated K280 tau was prepared and specificity characterized as described (Cohen *et al*., 2011). A polyclonal antibody specific for tau lacking acetylation at K280 (N-K280) was prepared using serum from rabbits immunized previously with a tau peptide spanning lysine 280 (VQIINKK) and a double affinity purification was performed (Thermo Scientific), in which acetylated K280-immunoreactive antibodies were depleted from serum prior to enrichment for the non-acetylated K280 antibody. Specificity was determined by western blotting of acetylated and non-acetylated K18 tau (data not shown). Other tau-specific monoclonal antibodies (Wolozin *et al*., 1986; Kosik *et al*., 1988; Novak *et al*., 1989; Mercken *et al*., 1992; Otvos *et al*., 1994; Seubert *et al*., 1995; Jicha *et al*., 1997*a*, *b*; Ghoshal *et al*., 2002; de Silva *et al*., 2003; Guillozet-Bongaarts *et al*., 2005) used in this study

Table 1 Summary of patient demographics

Neuropathological diagnosis	*n*	Age, years (SD)	Sex (F/M)	PMI (SD)	Brain weight, g (SD)
Alzheimer's disease (Braak V and VI)	11	75.2 (7.8)	(5/6)	10.5 (6.8)	1132.5 (131.8)
Alzheimer's disease (Braak III and IV)	5	79.6 (5.3)	(2/3)	8.9 (4.4)	1184.2 (154.5)
Normal (Braak I and II)	5	74.2 (11.0)	(3/2)	11.1 (6.0)	1264.8 (175.8)
Progressive supranuclear palsy	5	76.6 (9.6)	(1/4)	12 (5.7)	1257.6 (200.0)
Corticobasal degeneration	5	64.8 (14.6)	(1/4)	11.7 (5.7)	1071 (114.8)

PMI = post-mortem interval from death to autopsy (hours); SD = standard deviation.

Table 2 Tau-specific antibodies employed

Antibody	Type	Class	Epitope	Dilution	Source	Reference
Ac-K280	Polyclonal (affinity purified)	NA	ac-K280	1:250–500	CNDR	Cohen *et al*., 2011
N-K280	Polyclonal (affinity purified)	NA	Unmodified K280	3.3 mg/ml	CNDR	This study
Alz 50	Monoclonal (supernatant)	IgM	amino acids 5–15;312–322 (conformation)	1:100–500	Dr P Davies	Wolozin *et al*., 1986
MC1	Monoclonal (supernatant)	IgG^{1}	amino acids 5–15;312–322 (conformation)	1:100	Dr P Davies	Jicha *et al*., 1997*a*
MN423	Monoclonal (supernatant- purified)	IgG^{2b}	t-E391	1:200 000–250 000	Dr M Novak	Novak *et al*., 1989
TG3	Monoclonal (supernatant)	IgM	p-thr231 (conformation)	1:500	Dr P Davies	Jicha *et al*., 1997*b*
RD4	Monoclonal (supernatant- purified)	IgG	amino acids 275–291	1:10 000	Millipore	de Silva *et al*., 2003
PHF-1	Monoclonal (supernatant)	IgG^{1}	p- ser396, 404	1:500–1000	Dr P Davies	Otvos *et al*., 1994
AT8	Monoclonal (supernatant- purified)	IgG^{1}	p-ser199,202,thr205	1:500	Thermo Scientific	Mercken *et al*.,1992
AT100	Monoclonal (supernatant- purified)	IgG^{1}	p-thr212,ser214	1:500	Thermo Scientific	Mercken *et al*.,1992
12E8	Monoclonal (ascites-purified)	IgG	p-ser262, ser356	1:10 000	Elan Pharm.	Seubert *et al*., 1995
Tau 12	Monoclonal (supernatant- purified)	IgG^{1}	amino acids 9–18 (N-terminus)	1:10 000	Covance	Ghoshal *et al*., 2002
T46.1	Monoclonal (supernatant- purified)	IgG^{1}	amino acids 428–441 (C-terminus)	1:50 000	CNDR	Kosik *et al*., 1988
Tau-C3	Monoclonal (supernatant- purified)	IgG^{1}	t-D421	1:5000	Dr LI Binder	Guillozet-Bongaarts *et al*., 2005

ac = acetylation; p- = phosphorylation; t = truncation; NA = not available.

are summarized in Table 2. All primary antibodies were incubated overnight at 4°C, and species-specific biotinylated secondary antibodies were incubated for 1 h at room temperature as described (Forman *et al*., 2006; Cohen *et al*., 2011).

Double-label immunofluorescence was performed using these primary antibodies, and also a monoclonal antibody specific for glial fibrillary acidic protein (CNDR). Alexa Fluor 488 and 594 species-specific conjugated secondary antibodies (Molecular Probes) were incubated overnight at 4°C. Slides were treated for autofluorescence using a 0.3% Sudan Black solution and cover-slipped with Vectashield-DAPI mounting medium (Vector Laboratories). Double-label immunofluorescence experiments using thioflavin-S and polyclonal antibody against acetylated K280 were first stained with thioflavin-S, followed by overnight incubation with the acetylated K280 polyclonal antibody, as described (Cohen *et al*., 2011).

Digital images of immunohistochemical results were obtained using an Olympus BX 51 microscope equipped with a bright-field and fluorescence light source with a DP-71 digital camera (Olympus) and DP manager software (Olympus). Digital images for immunofluorescence experiments were overlaid into a merge channel using Adobe Photoshop, version 9.0.2 (Adobe Systems).

Microscopic and statistical analysis

Regional distribution of acetylated K280 immunoreactive was assessed in 30 representative cortical and subcortical regions (Fig. 1 and Supplementary Figs 1 and 2). These regions were examined with direct comparison of acetylated K280 immunoreactive to paired-helical filament-1-immunoreactive for each case using a semi-quantitative scale for overall burden of tau pathology (0 = none, 1 = mild, 2 = moderate, 3 = severe). Scoring was based on the area of highest severity in each slide. The median semi-quantitative score for each region was calculated from grouped data from all patient cases in each disease group (SPSS 15.0, SPSS).

Quantification of acetylated K280-immunoreactive neurofibrillary tangles was performed on digital images from three semi-random

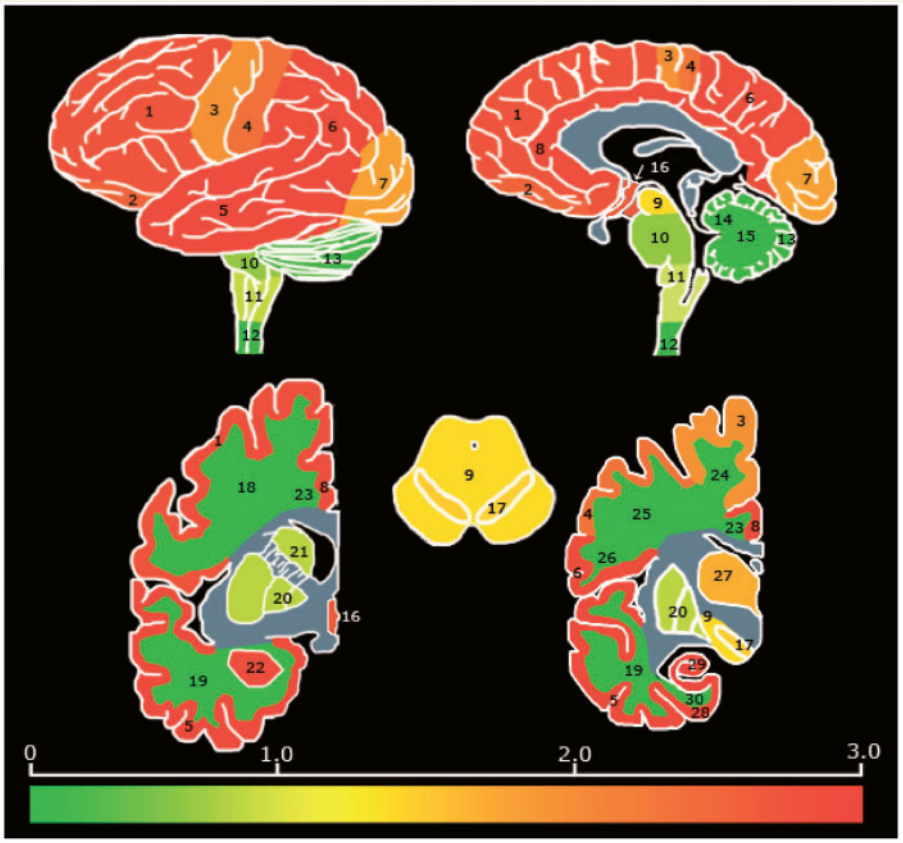

Figure 1 Regional distribution and severity of acetylated K280 pathology in patients with Alzheimer's disease. Heat map of acetylated K280-immunoreactivity pathology in the CNS of patients with Alzheimer's disease (n = 10) based on median severity scores for grouped data per region. Regional distribution was typical for Alzheimer's disease, with greatest severity in limbic and cortical grey matter. Bar graph depicts colour map of severity score ranging from no pathology (0 = green) to severe (3 = red). Blue regions were not evaluated. Brain regions evaluated include: 1 = midfrontal cortex grey matter; 2 = oribitofrontal cortex grey matter; 3 = motor cortex grey matter; 4 = sensory cortex grey matter; 5 = superior/mid temporal cortex grey matter; 6 = angular cortex grey matter; 7 = visual cortex grey matter; 8 = anterior cingulate cortex grey matter; 9 = midbrain; 10 = pons; 11 = medulla; 12 = cervical spinal cord; 13 = cerebellar cortex; 14 = cerebellar white matter; 15 = dentate nucleus; 16 = hypothalamus; 17 = substantia nigra; 18 = mid frontal cortex white matter; 19 = superior/mid temporal cortex white matter; 20 = lentiform nucleus; 21 = striatum; 22 = amygdala; 23 = anterior cingulate gyrus white matter; 24 = motor cortex white matter; 25 = sensory cortex white matter; 26 = angular cortex white matter; 27 = thalamus; 28 = entorhinal cortex grey matter; 29 = hippocampal formation (cornu ammonis 1–4/subiculum); and 30 = entorhinal cortex white matter.

(alternating non-overlapping) 0.14 mm^2 fields of view in the cornu ammonis (CA-1) region of the hippocampus in the 10 Braak V and VI Alzheimer's disease cases double labelled with Alz50, MN423, thioflavin-S or glial fibrillary acidic protein. One case used in the regional analysis had limited hippocampal tissue available and was replaced with an equivalent Alzheimer's disease case for this analysis. Quantification of acetylated K280-immunoreactive tangles co-labelled with thioflavin-S or these monoclonal antibodies were expressed as an average percentage of acetylated K280-immunoreactive inclusions with double fluorescence per 0.14 mm^2 and standard deviation.

To further study the potential role for acetylated K280 in tangle development, adjacent or closely matched sections were examined from the hippocampal formation of five cases each of Braak Stages I–VI. Morphological subtypes of neurofibrillary tangles (pre-tangles, intracellular tangles and extracellular ghost tangles) were determined based on previous descriptions (Schmidt *et al*., 1988; Garcia-Sierra *et al*., 2001; Augustinack *et al*., 2002; Lauckner *et al*., 2003). Tangle counts of these subtypes were performed on digital images of three semi-random (alternating non-overlapping) 0.14 mm^2 fields in the CA-1 region for each case and antibody (acetylated K280, Alz50, MN423 and paired-helical filament-1) and recorded. The severity of dystrophic neurites detected by each antibody in these fields of view was also assessed using a (0–3) semi-quantitative scale based on a previous report (Mukaetova-Ladinska *et al*., 1993). Average scores for neuritic staining per case were calculated for each antibody. This analysis was additionally performed in another five cases of severe (Braak V and VI) Alzheimer's disease hippocampus with acetylated K280 and the 4R-specific tau epitopes, RD4 and non-acetylated K280. Comparisons between neurofibrillary tangles and neurites detected by acetylated K280 and other tau-specific antibodies per Alzheimer's disease Braak stage were compared using a Wilcoxon signed-rank comparison. The average tangle count or neuritic score per case for monoclonal antibodies paired-helical filament1, Alz50 and MN423 were subtracted from acetylated K280 values and reported as median difference with the interquartile range 25–75 percentile.

Results

Regional distribution

Significant acetylated K280 immunoreactivity was observed in pathological inclusions in all cases examined. Acetylated-K280 immunoreactivity displayed a similar distribution and pathological burden to hyperphosphorylated tau, using the monoclonal antibody paired-helical filament-1, in Alzheimer's disease (Fig. 1), progressive supranuclear palsy and corticobasal degeneration (Supplementary Figs 1 and 2). There were no brain regions where acetylated K280 immunoreactivity was seen in the absence of paired-helical filament-1-immunoreactive tau pathology. In some cases, regions with rare paired-helical filament-1-immunoreactive inclusions had no acetylated-K280-immunoreactive tangles, while in most severely affected regions the acetylated-K280-immunoreactive tangle burden was similar to paired-helical filament-1-immunoreactivity (Supplementary Tables 1–3).

Morphological features of acetylated K280-immunoreactive tau pathology

The acetylated K280 polyclonal antibody stained all key pathological inclusions in Alzheimer's disease, corticobasal degeneration and progressive supranuclear palsy, including neurofibrillary tangles, neuropil threads and neuritic plaques in Alzheimer's disease, tufted astrocytes, coiled bodies and globose tangles in progressive supranuclear palsy, and astrocytic plaques, coiled bodies and ballooned neurons in corticobasal degeneration (Fig. 2). Smaller, diffuse threads were less prominent in acetylated K280-stained sections for all diseases. This difference was most evident in Alzheimer's disease, where neuropil threads were minimal compared with paired-helical filament-1 staining. This is in contrast to the similar levels of acetylated-K280-immunoreactive neurofibrillary tangles and large dystrophic neurites associated with neuritic plaques. This observation was consistent when immunohistochemistry was performed at multiple dilutions of the primary antisera and with several different antigen retrieval methods (data not shown). Interestingly, quantification of cortical layer II neurofibrillary tangles in cases with corticobasal degeneration showed less acetylated K280 immunoreactivity than paired-helical filament-1-immunoreactive lesions (Supplementary Table 4), while acetylated K280-immunoreactive astrocytic plaques in corticobasal degeneration and neuronal reactivity in globose tangles of progressive supranuclear palsy cases were comparable with paired-helical filament-1 (Fig. 2).

The most robust acetylated-K280 immunoreactivity was observed in Alzheimer's disease intracellular tangles. A subset of these neurofibrillary tangles appeared granular and non-confluent, resembling pre-tangles; however, the majority were mature intracellular neurofibrillary tangles.

Since the acetylated K280 epitope is located in the second microtubule-binding repeat, and is specific for 4R tau isoforms, and 4R tau specific antibodies also detect intracellular neurofibrillary tangles but to a lesser extent neuropil threads (Yoshida, 2006) and ghost tangles (Yoshida, 2006; Espinoza *et al*., 2008), we compared serial sections of hippocampus from cases with Braak Stage V and VI Alzheimer's disease ($n = 5$) stained with acetylated K280, affinity-purified antisera specific for the non-acetylated K280 epitope, and a 4R-specific monoclonal antibody (RD4) to determine the distribution of acetylated and non-acetylated K280, as well as E10, in neurofibrillary tangles. As shown in Fig. 3, both non-acetylated K280 and RD4 stained more neuropil threads than acetylated K280 ($P < 0.05$), although all three antibodies detected neurofibrillary tangles to a similar extent (Table 3). The higher level of neuropil thread reactivity with these monoclonal antibodies illustrates the unique pathological signature of acetylated K280, compared with non-acetylated (N-K280) and total (RD4) 4R-tau.

Comparison with tau epitopes across varying stages of Alzheimer's disease severity

Previous studies have used anti-tau and anti-neurofibrillary tangle antibodies to document the evolution of neurofibrillary tangles by comparing the emergence and sequential appearance of hyperphosphorylation, conformational changes, and C- and N-terminal tau truncation neoepitopes in Alzheimer's disease brains at different Braak stages (Garcia-Sierra *et al*., 2003; Guillozet-Bongaarts *et al*., 2005; Luna-Munoz *et al*., 2005; Mondragon-Rodriguez *et al*., 2008). These studies provide a model of tangle progression, with some epitopes being present in earlier forms of pathology (i.e. pre-tangles), and are mutually exclusive to 'late' epitopes seen mostly in intracellular and ghost tangles.

To determine when acetylation of K280 occurs during neurofibrillary tangle development, we examined serial sections of Alzheimer's disease hippocampus from varying stages of disease with several well characterized tau antibodies. The monoclonal antibody Alz50 (Wolozin *et al*., 1986; Carmel *et al*., 1996), a conformation-specific epitope, previously shown to occur early in neurofibrillary tangle formation due to its presence in early Alzheimer's disease cases (Mena *et al*., 1991) and co-localization with antibodies specific to the intact N- and C-terminal tau residues (Garcia-Sierra *et al*., 2003) was chosen as an early stage neurofibrillary tangle marker. On the other hand, MN423 (Wischik *et al*., 1988; Novak *et al*., 1989, 1991), an antibody specific for the C-terminal truncation of tau at Q391, was chosen as a late stage neurofibrillary tangle marker since it recognizes a neoepitope in neurofibrillary tangles (Novak *et al*., 1993) and reacts well with extracellular tangles (Garcia-Sierra *et al*., 2001). Paired-helical filament-1 was also included in the analysis, as hyperphosphorylation at S396/404 is thought to predate conformational and truncation steps (Garcia-Sierra *et al*., 2003).

Analysis of these sections showed acetylated K280 detected a majority of intracellular neurofibrillary tangles (Supplementary Fig. 3), and there was consistently less neuritic staining with acetylated K280 than Alz50 and paired-helical filament-1 throughout all stages of disease ($P < 0.05$, Braak III and VI) (Tables 4 and 5). Analysis of the median difference in the average tangle count per field between acetylated K280 immunoreactivity and the other tau antibodies showed that acetylated K280-immunoreactive

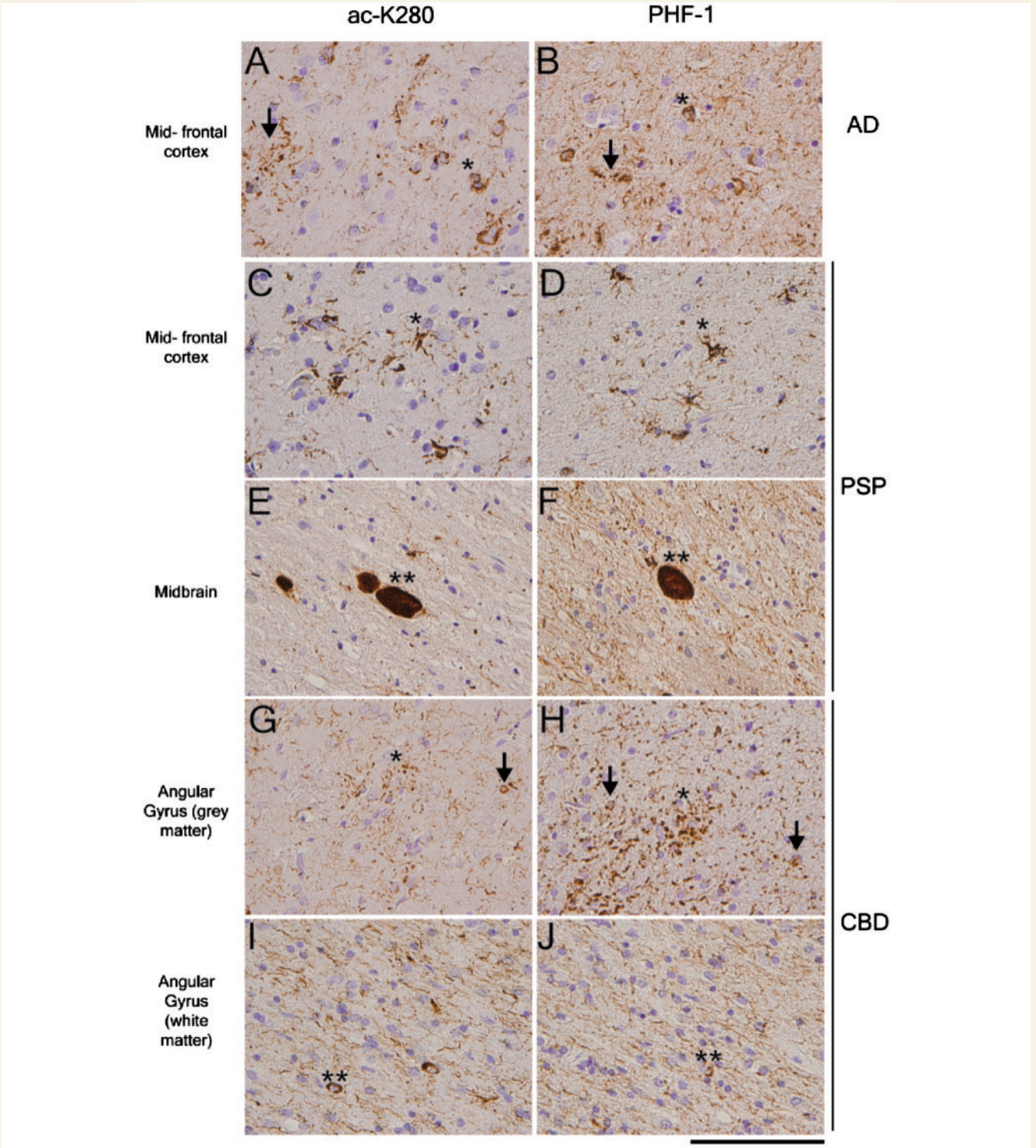

Figure 2 Acetylated-K280 reactive pathology in the major 4-R tau isoform containing tauopathies. Mid-temporal cortex sections from an Alzheimer's disease (AD) case (**A** and **B**) immunostained with acetylated K280 (ac-K280; **A**) show key aspects of tau pathology including neurofibrillary tangles (asterisk), neuritic plaques (arrow) and neuropil threads. Compared with paired-helical filament-1-immunoreactivity (**B**), there is similar numbers of tangles with a lower density of neuropil threads. Midfrontal cortex (**C** and **D**) and midbrain (**E** and **F**) sections from a case with progressive supranuclear palsy (PSP) immunostained with acetylated K280 (**C** and **E**) showed characteristic tau pathologic inclusions tufted astrocytes (asterisk) and globose tangles (double asterisk). Compared with paired-helical filament-1-immunoreactivity (**D** and **F**) there was similar acetylated K280 reactivity in neuronal and compact glial inclusions. Angular gyrus grey (**G** and **H**) and white matter (**I** and **J**) sections from a case of corticobasal degeneration (CBD) immunostained with acetylated K280 (**G** and **I**) showing similar reactivity of astrocytic plaques (asterisk) and coiled bodies (double asterisk) with minimal reactivity in layer II neuronal tangles (arrows) compared with paired-helical filament-1-immunoreactivity (**H** and **J**). Scale bar = 100 μm.

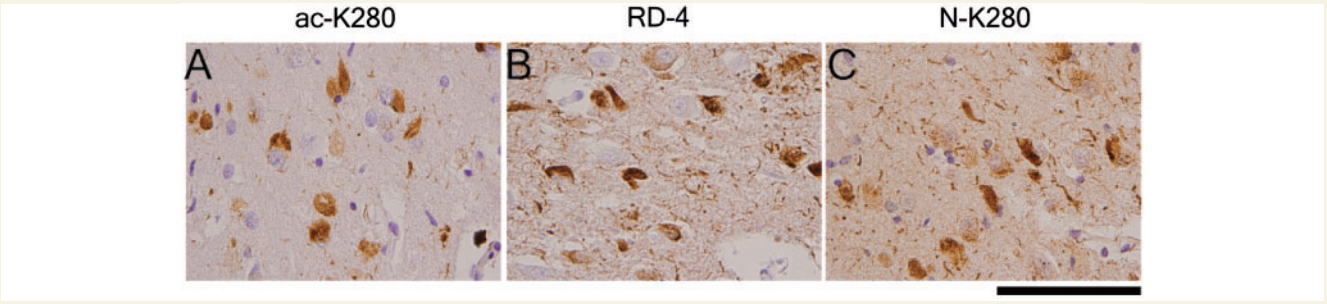

Figure 3 Comparison of acetylated K280-immunoreactive inclusion morphology with 4R tau-specific antibodies. Serial sections of Alzheimer's disease cornu ammonis region 1 stained with (**A**) acetylated K280m ac-K280, (**B**) the 4R-tau isoform-specific tau antibody, RD-4, and (**C**) affinity purified antisera specific for non-acetylated tau at residue K280 (N-K280). The predominance of intracellular tangles with minimal neuropil thread pathology seen in acetylated K280 is not evident using other 4R-specific antisera, confirming this unique morphology is due to the preferential expression of acetylated K280 tau in these lesions. Scale bar = 100 μm.

Table 3 Quantification of neurofibrillary pathology detected by 4R tau isoform-dependent antibodies in the Alzheimer's disease hippocampus

Antibodies												
Alzheimer's disease stage	Acetylated-K280				RD4				Non-acetylated K280			
	Pre-tangle	Tangle	Ghost tangle	Neurite score	Pre-tangle	Tangle	Ghost tangle	Neurite score	Pre-tangle	Tangle	Ghost tangle	Neurite score
Braak V–VI	0.7 ± 0.8	10.9 ± 3.3	1.3 ± 0.9	1 (0.25,1)*	1.5 ± 1.2	11.0 ± 1.9	0.7 ± 0.8	2 (2–2)	0.7 ± 01.0	11.3 ± 2.5	1.4 ± 0.8	2 (2–2)

Values are average ± standard deviation of lesion count in 0.14 mm^2 field of cornu ammonis region-1 of hippocampus ($n = 5$ cases). Neurite score represents the median value for neuropil thread staining per 0.14 mm^2 field (interquartile range 25–75 percentile).
*$P < 0.05$ for comparison of acetylated-K280 neurite score to both RD4 and non-acetylated K280 neurite score (Wilcoxon signed-rank test).

neurofibrillary tangles were less apparent than paired-helical filament-1 ($P < 0.05$) or Alz50 staining in early Alzheimer's disease stages and similar to paired-helical filament-1 in intermediate and late Alzheimer's disease stages (Table 5). Acetylated-K280-immunoreactive intracellular tangles were more abundant in later Alzheimer's disease stages than those detected by MN423 ($P < 0.05$) and Alz50, and also displayed fewer pre-tangles than Alz50 ($P < 0.05$), and fewer ghost tangles than MN423 ($P < 0.05$) (Table 5). Examination of layer II of entorhinal cortex showed distinctive populations of ghost tangles (Garcia-Sierra *et al*., 2001), which were highly reactive to paired-helical filament-1 and MN423 and minimally reactive in acetylated K280 stained sections (Supplementary Fig. 3). Thus, acetylated K280 immunoreactivity appears to occur later in relation to Alz50 and paired-helical filament-1-immunoreactivity, and earlier than MN423, with a predominance of reactivity in intracellular neurofibrillary tangles.

Co-localization of acetylated K280 immunoreactivity with multiple tau epitopes in Alzheimer's disease

To confirm these observations of acetylated K280 immunoreactivity occurring as a relatively early intermediate between Alz50 and MN423 epitopes, double labelling experiments were performed using these monoclonal antibodies and thioflavin-S staining, which binds tau amyloid. Examination of the CA-1 region in Braak V and VI cases showed almost exclusive co-localization of acetylated K280 immunoreactive with thioflavin-S positive tangles (average 97.8 ± 2.3%) (Fig. 4), while some thioflavin-S-positive neurofibrillary tangles were not acetylated K280 immunoreactive. The majority of these thioflavin-S-positive, acetylated K280 negative inclusions resembled extracellular ghost tangles, which are released from dying tangle bearing neurons (Schmidt *et al*., 1988). Since these extracellular neurofibrillary tangles induce gliosis they display glial fibrillary acidic protein-immunoreactivity (Schmidt *et al*., 1988; Ikeda *et al*., 1992) and Braak Stage V and VI Alzheimer's disease cases showed co-localization of acetylated K280 immunoreactive with glial fibrillary acidic protein immunoreactive ghost tangles. The extent of this co-localization varied considerably from case to case, with an average overlap of 18.1 ± 11.6% (Fig. 4). Co-localization of acetylated K280-immunoreactive neurofibrillary tangles was moderate for Alz50 (72.6 ± 5.5%) and was less evident for MN423 (30.7 ± 9.1%) (Fig. 4). Both monoclonal antibodies displayed mutually exclusive tangles that were either Alz50/MN423-immunoreactive or acetylated K280 immunoreactive only. The majority of exclusive MN423-immunoreactivity appeared to be predominantly ghost tangles. Thus, it appears that tau acetylation is found mostly in

Table 4 Quantification of neurofibrillary pathology detected by ac-K280 and other tau epitopes throughout various stages of Alzheimer's disease pathology

Antibodies														
Alzheimer's disease stage	PHF-1				Alz50			Ac-K280			MN423			
	Pre-tangle	Tangle	Ghost tangle	Neurite score	Pre-tangle	Tangle	Ghost tangle	Neurite score	Pre-tangle	Tangle	Ghost tangle	Neurite score	Pre-tangle	Tangle	Ghost tangle	Neurite score
Braak I and II	0.2 ± 0.7	1.1 ± 1.6	0.0 ± 0.3	1 (0–1.5)	0.4 ± 1.4	0.7 ± 0.9	0.0 ± 0.0	1 (0–1)	0.1 ± 0.4	0.4 ± 1.0	0.0 ± 0.0	0 (0–0)	0.0 ± 0.0	0.0 ± 0.3	0.1 ± 0.4	0 (0–0)
Braak III and IV	2.0 ± 2.1	4.1 ± 1.9	0.5 ± 0.7	3 (2–3)	2.3 ± 1.7	2.3 ± 1.2	0.1 ± 0.3	2 (2–3)	0.3 ± 0.5	2.7 ± 3.1	0.1 ± 0.3	0 (0–0)	0.0 ± 0.0	0.9 ± 1.0	1.7 ± 1.8	0 (0–0)
Braak V and VI	1.3 ± 0.8	14.7 ± 3.1	1.8 ± 1.5	3 (3–3)	5.4 ± 3.3	6.9 ± 3.7	0.1 ± 0.4	3 (3–3)	0.5 ± 0.9	11.8 ± 1.9	1.8 ± 1.0	1 (0–1)	0.0 ± 0.0	3.5 ± 1.3	4.5 ± 3.5	0 (0–1)

Values represent average ± SD of lesion count in 0.14 mm^2 field of cornu ammonis region-1 of hippocampus ($n = 5$ cases). Neurite score represents the median value for neuropil thread staining per 0.14 mm^2 field (interquartile range 25–75 percentile).

intracellular thioflavin-S-positive neurofibrillary tangles, and to a lesser extent in granular pre-tangles and extracellular ghost tangles. In addition, it appears to represent an intermediate stage between the early Alz50 and late MN423 epitopes.

Acetylated K280 immunoreactivity was also compared with several other phosphorylation- and conformation-dependent tau antibodies examined (Supplementary Fig. 4) and co-localized well with neurofibrillary tangles with these antibodies and only weakly in neurites. There were occasional exclusively labelled tangles for all antibodies tested, indicating a dynamic process of epitope expression in tangle progression. Thus, acetylated K280 was co-expressed in a significant proportion of intracellular tangles for all antibodies tested.

Discussion

Using the acetylated K280 tau specific polyclonal antibody, we thoroughly evaluated diverse CNS regions in a large number of Alzheimer's disease, progressive supranuclear palsy and corticobasal degeneration cases with a detailed examination of Alzheimer's disease hippocampus throughout various Braak stages of disease. We demonstrate that acetylated K280 immunoreactivity is a significant marker of tau pathology in 4R tauopathies including Alzheimer's disease, corticobasal degeneration and progressive supranuclear palsy. Significantly, the acetylated K280 tau epitope was consistently found in the tau pathology of all cases studied, and it followed a similar distribution and regional severity to that of hyperphosphorylated tau epitopes. Moreover, we determined a potential temporal sequence for acetylation at K280 of tau in the process of tangle development. These findings provide insight into the role of acetylation in tangle formation.

Comparison of the acetylated K280-immunoreactive tau pathology burden to phosphorylated tau-immunoreactive pathology within cases generally showed similarity in more severely affected areas. Assuming that less severely affected areas would have a predominance of early pathology; tau hyperphosphorylation may precede acetylation at the K280 residue, mirroring our data from examination of early Braak stages. Interestingly, most phosphorylation sites occur in regions flanking the microtubule-binding repeat (Buee *et al.*, 2000), in which K280 is located. Perhaps, hyperphosphorylation renders this residue available for subsequent acetylation, which would further impair microtubule binding and/or promote tau aggregation as well as further drive pathological alterations of tau.

Additionally, the minimal pre-tangle reactivity and weak co-localization of acetylated K280 immunoreactivity in neuropil threads labelled by phosphorylation-dependent monoclonal antibodies support this observation, since neuropil threads are thought to emerge earlier than neurofibrillary tangles (Ghoshal *et al.*, 2002). This should be interpreted with the caveat that the potential tau de-acetylase enzyme HDAC-6, (Cohen *et al.*, 2011) is noted to be highly expressed in the cytoplasm of neurons in Alzheimer's disease cases (Miki *et al.*, 2011). Thus, the minimal neuritic staining observed here with acetylated K280 immunoreactivity may be a reflection of increased de-acetylase activity in neuronal processes that could abolish this epitope.

Table 5 Difference in neurofibrillary pathology detected by acetylated K280 and other tau epitopes throughout various stages of Alzheimer's disease pathology

Epitope	Braak I and II	Braak III and IV	Braak V and VI
ac-K280- PHF1 tangles	−0.67 (−1.34 to −0.67)*	−1.67 (−2.33 to −1.67)	−2.67 (−4 to −0.33)
ac-K280-PHF1 pre-tangles	0 (0 to 0.33)	−1 (−3.33 to −0.67)	−0.67 (−1.33 to −0.033)
ac-K280-PHF1 ghost tangles	0 (0 to 0)	0 (−0.67 to 0)	0.33 (−0.34 to 0.33)
ac-K280-PHF1 neurite score	−1 (−1.33 to 0)	−2.67(−3 to −1.67)*	−2.33(−2.67 to −2.33)*
ac-K280-Alz 50 tangles	−0.33 (−0.34 to 0)	−0.66 (−0.66 to 1)	7.34 (2.67 to 7.67)
ac-K280-Alz50 pre-tangles	0 (0 to 0)	−2.33 (−3 to −0.67)*	−5 (−7 to −3.33)*
ac-K280-Alz 50 ghost tangles	0 (0 to 0)	0 (0 to 0)	1.33 (1 to 2)*
ac-K280-Alz50 neurite score	−1 (−1 to 0)	−2 (−2.33 to −1.33)*	−2.33 (−2.67, −2.33)*
ac-K280-MN423 tangles	0.33 (0 to 0.33)	0.67 (0.34 to 2.33)*	9.33 (7.67 to 9.66)*
ac-K280-MN423 pre-tangles	0 (0 to 0.33)	0.33 (0 to 0.33)	0 (0 to 1)
ac-K280-MN423 ghost tangles	0 (0 to 0)	−0.67 (−2.67 to −0.33)*	−2.34 (−5 to −1)*
ac-K280-MN423 neurite score	0 (0 to 0)	0 (0 to 0.33)	0 (−0.33 to 0.33)

Values displayed are median (interquartile range 25–75 percentile) difference in average acetylated-K280-immunoreactive tangle count/neurite score and respective tau epitope.
*$P < 0.05$ Wilcoxon signed-rank test. Ac-K280 = acetylated-K280; PHF = paired-helical filaments.

The most striking feature of acetylated K280 immunoreactivity in Alzheimer's disease was the prominent detection of intracellular tangles. This finding was evidenced by the almost exclusive co-localization of acetylated K280 immunoreactivity with thioflavin–S-positive neurofibrillary tangles, but not in neuropil threads detected by thioflavin-S or multiple other anti-tau antibodies examined here. Indeed, acetylated K280 was mostly associated with intracellular neurofibrillary tangles compared to pre-tangles or extracellular ghost tangles throughout all Braak stages. Similar findings have been reported for conformational and truncation tau epitopes that are thought to represent intermediate stages of tangle progression (Garcia-Sierra *et al*., 2003; Guillozet-Bongaarts *et al*., 2005). However, unlike these epitopes, acetylated K280 also co-localized with N- and C-terminal specific anti-tau epitopes (Supplementary Fig. 4), indicating it is present in neurofibrillary tangles prior to subsequent tau truncation. This is supported by our observations that acetylated K280 immunoreactivity did not co-localize well with the truncation-specific tau epitope, MN423 and detected less glial fibrillary acidic protein-immunoreactive ghost tangles. Interestingly, the variability in acetylated K280 immunoreactive ghost tangles suggests that de-acetylation of K280 could occur when neurofibrillary tangles are released into the extracellular space from dying tangle bearing neurons. Another possibility is masking of the epitope in the paired-helical filament core, although prolonged antigen retrieval steps did not reveal additional extracellular tangle staining. In this regard, acetylated K280 was similar to the early Alz50 epitope, in that both antibodies did not detect many extracellular ghost tangles; however, there was only partial co-localization with Alz50, especially for early pre-tangle structures, and acetylated K280 immunoreactivity outnumbered Alz50 in neurofibrillary tangles in cases with severe Alzheimer's disease as this epitope was lost due to truncation events.

These data suggest that acetylation of K280 may be an intermediate step in tangle formation from threads and pre-tangle structures, which predominate in Alz50-immunoreactivity, is most associated with thioflavin-S-positive intracellular neurofibrillary tangles, and lost prior to the emerge of the majority of extracellular ghost tangles detected by MN423-immunoreactivity and glial fibrillary acidic protein-immunoreactivity.

Although pathological tau lesions in corticobasal degeneration and progressive supranuclear palsy do not react with amyloid-binding dyes (Dickson, 2004) such as thioflavin-S, and are thought to contain less post-translational modifications than in Alzheimer's disease (Arai *et al*., 2003), they were robustly positive for acetylated K280. These tauopathies have minimal extracellular tau pathology, and several late tau epitopes are not present in corticobasal degeneration and progressive supranuclear palsy cases (Berry *et al*., 2004; Guillozet-Bongaarts *et al*., 2005), further suggesting that acetylated K280 may precede tau-amyloid formation and late truncation events. The minimal acetylated K280 immunoreactivity in neuronal lesions in superficial layers of corticobasal degeneration cortical sections is intriguing, and may suggest alternative pathological cascades of tau modifications in differing cell types. Indeed, others have also shown a dissociation of tau epitope expression between cell types in these tauopathies (Guillozet-Bongaarts *et al*., 2007).

Our data presented here suggest that acetylation of K280 in tau could play a mechanistic role in driving tau polymerization into neurofibrillary pathology and tau mediated neurodegeneration. We also previously identified three other potential tau acetylation sites, two of which are also in the microtubule-binding repeat (Cohen *et al*., 2011). Further examination of these epitopes may also suggest a potential dynamic interplay between acetylation and phosphorylation at multiple sites that may act synergistically in the pathogenesis of tau fibrillization. Thus, a better

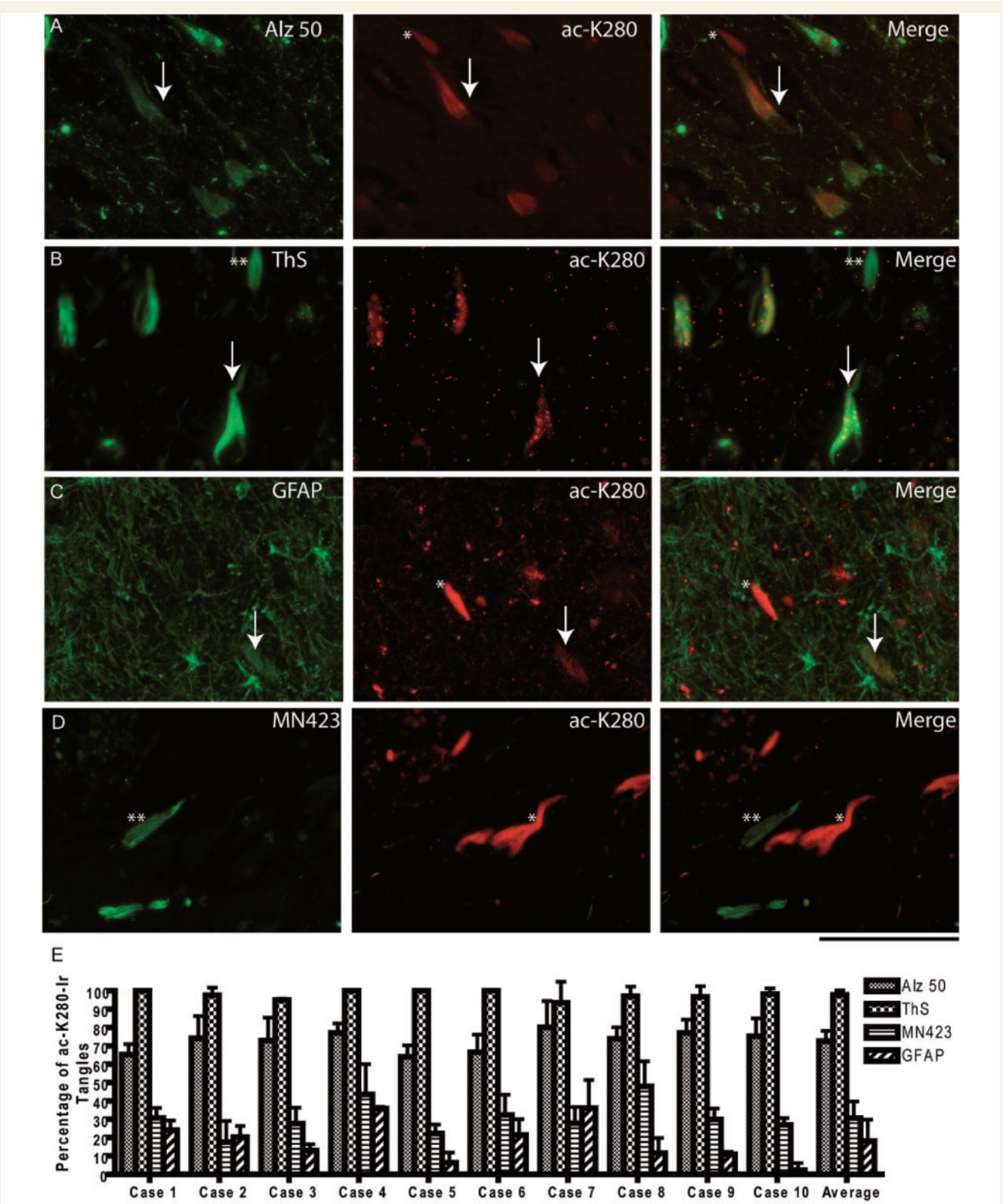

Figure 4 Quantification of co-localization of acetylated-tau pathology in Alzheimer's disease neurofibrillary tangles. (**A**) Double-label experiments of the cornu ammonis region 1 (CA-1) pyramidal neurons showing moderate levels of co-localization (arrow) between the early Alz50 epitope and acetylated K280, with a subset of exclusively acetylated K280-immunoreactive neurofibrillary tangles (asterisk). (**B**) The majority of acetylated K280-immunoreactive tangles co-localized to thioflavin-S (ThS)-positive neurofibrillary tangles (arrow), with some exclusively thioflavin-S-labelled neurofibrillary tangles (double asterisk). (**C**) Co-localization of glial fibrillary acidic protein (GFAP)-immunoreactive ghost tangles in a subset of acetylated K280-immunoreactive tangles (arrow), with exclusively acetylated K280-immunoreactive intracellular neurofibrillary tangles (asterisk). (**D**) Co-localization was less evident for acetylated K280 and the late

(continued)

understanding of the relationship of these post-translational modifications could be crucial to identify potential targets for therapy in Alzheimer's disease and other tauopathies, as well as biomarker development using acetylation-specific antibodies such as the acetylated K280 polyclonal antibody studied here. Although further work is required in cell and animal models to elucidate a possible functional role of tau acetylation in the pathogenesis of neurofibrillary tangles, such insights will advance efforts to test whether disruption of this process could prevent cell death and alter disease progression.

Acknowledgements

We would like to thank Drs Anjan Chatterjee, Christopher Clark, Amy Colcher, H. Branch Coslett, John Duda, Stacy Horn, Howard I. Hurtig and Jason Karlawish, for contribution of clinical information for patients used in this study and Andrew Hwang, Dr David Hurtado and Dr Felix Geser for their assistance. We would also like to thank Dr. Peter Davies (paired-helical filament-1, Alz50, MC1 and TG3), Dr Lester I. Binder (Tau-C3) and Dr Michal Novak (MN423) for their kind gift of these monoclonal antibodies used in our study.

Funding

National Institutes of Health (P30 AG010124-20) Alzheimer's disease core centre grant. National Institutes of Health (T32-AG000255 to D.J.I.) training grant.

Supplementary material

Supplementary material is available at *Brain* online.

References

Arai T, Ikeda K, Akiyama H, Tsuchiya K, Iritani S, Ishiguro K, et al. Different immunoreactivities of the microtubule-binding region of tau and its molecular basis in brains from patients with Alzheimer's disease, Pick's disease, progressive supranuclear palsy and corticobasal degeneration. Acta Neuropathol 2003; 105: 489–98.

Augustinack JC, Schneider A, Mandelkow EM, Hyman BT. Specific tau phosphorylation sites correlate with severity of neuronal cytopathology in Alzheimer's disease. Acta Neuropathol 2002; 103: 26–35.

Berry RW, Sweet AP, Clark FA, Lagalwar S, Lapin BR, Wang T, et al. Tau epitope display in progressive supranuclear palsy and corticobasal degeneration. J Neurocytol 2004; 33: 287–95.

Biernat J, Gustke N, Drewes G, Mandelkow EM, Mandelkow E. Phosphorylation of Ser262 strongly reduces binding of tau to microtubules: distinction between PHF-like immunoreactivity and microtubule binding. Neuron 1993; 11: 153–63.

Bramblett GT, Goedert M, Jakes R, Merrick SE, Trojanowski JQ, Lee VM. Abnormal tau phosphorylation at Ser396 in Alzheimer's disease recapitulates development and contributes to reduced microtubule binding. Neuron 1993; 10: 1089–99.

Braak H, Braak E. Neuropathological stageing of Alzheimer-related changes. Acta Neuropathol 1991; 82: 239–59.

Buee L, Bussiere T, Buee-Scherrer V, Delacourte A, Hof PR. Tau protein isoforms, phosphorylation and role in neurodegenerative disorders. Brain Res Brain Res Rev 2000; 33: 95–130.

Carmel G, Mager EM, Binder LI, Kuret J. The structural basis of monoclonal antibody Alz50's selectivity for Alzheimer's disease pathology. J Biol Chem 1996; 271: 32789–95.

Cohen TJ, Guo JL, Hurtado DE, Kwong LK, Mills IP, Trojanowski JQ, et al. The acetylation of tau inhibits its function and promotes pathological tau aggregation. Nat Commun 2011; 2: 252.

de Silva R, Lashley T, Gibb G, Hanger D, Hope A, Reid A, et al. Pathological inclusion bodies in tauopathies contain distinct complements of tau with three or four microtubule-binding repeat domains as demonstrated by new specific monoclonal antibodies. Neuropathol Appl Neurobiol 2003; 29: 288–302.

Dickson D. Sporadic Tauopaties: Pick's disease, corticobasal degeneration, progressive supranuclear palsy and argyrophilic grain disease. In: Esiri M, Lee VM-Y, Trojanowski JQ, editors. The neuropathology of dementia. 2 edn. New York, NY: Cambridge University Press; 2004. p. 227–55.

Espinoza M, de Silva R, Dickson DW, Davies P. Differential incorporation of tau isoforms in Alzheimer's disease. J Alzheimers Dis 2008; 14: 1–16.

Forman MS, Farmer J, Johnson JK, Clark CM, Arnold SE, Coslett HB, et al. Frontotemporal dementia: clinicopathological correlations. Ann Neurol 2006; 59: 952–62.

Garcia-Sierra F, Ghoshal N, Quinn B, Berry RW, Binder LI. Conformational changes and truncation of tau protein during tangle evolution in Alzheimer's disease. J Alzheimers Dis 2003; 5: 65–77.

Garcia-Sierra F, Wischik CM, Harrington CR, Luna-Munoz J, Mena R. Accumulation of C-terminally truncated tau protein associated with vulnerability of the perforant pathway in early stages of neurofibrillary pathology in Alzheimer's disease. J Chem Neuroanat 2001; 22: 65–77.

Ghoshal N, Garcia-Sierra F, Wuu J, Leurgans S, Bennett DA, Berry RW, et al. Tau conformational changes correspond to impairments of episodic memory in mild cognitive impairment and Alzheimer's disease. Exp Neurol 2002; 177: 475–93.

Guillozet-Bongaarts AL, Garcia-Sierra F, Reynolds MR, Horowitz PM, Fu Y, Wang T, et al. Tau truncation during neurofibrillary tangle evolution in Alzheimer's disease. Neurobiol Aging 2005; 26: 1015–22.

Hoffmann R, Lee VM, Leight S, Varga I, Otvos L Jr. Unique Alzheimer's disease paired helical filament specific epitopes involve double phosphorylation at specific sites. Biochemistry 1997; 36: 8114–24.

Ikeda K, Akiyama H, Haga C, Haga S. Evidence that neurofibrillary tangles undergo glial modification. Acta Neuropathol 1992; 85: 101–4.

Jack CR Jr, Knopman DS, Jagust WJ, Shaw LM, Aisen PS, Weiner MW, et al. Hypothetical model of dynamic biomarkers of the Alzheimer's pathological cascade. Lancet Neurol 2010; 9: 119–28.

Jicha GA, Bowser R, Kazam IG, Davies P. Alz-50 and MC-1, a new monoclonal antibody raised to paired helical filaments, recognize

Figure 4 Continued

MN423 epitope with more frequent mutually exclusive neurofibrillary tangles (asterisk and double asterisk). Scale bar = 100 μm. (**E**) Bar graph depicts percentage of acetylated K280-immunoreactive tangles co-labelled with thioflavin-S and multiple tau epitopes in the CA-1 region of severe Alzheimer's disease cases (n = 10). Acetylated-K280 co-expression in tangles occurred most with thioflavin-S and appeared to represent an intermediate between early (Alz50) and late (MN423) tau epitopes.

conformational epitopes on recombinant tau. J Neurosci Res 1997a; 48: 128–32.

Jicha GA, Lane E, Vincent I, Otvos L Jr, Hoffmann R, Davies P. A conformation- and phosphorylation-dependent antibody recognizing the paired helical filaments of Alzheimer's disease. J Neurochem 1997b; 69: 2087–95.

Kosik KS, Orecchio LD, Binder L, Trojanowski JQ, Lee VM, Lee G. Epitopes that span the tau molecule are shared with paired helical filaments. Neuron 1988; 1: 817–25.

Lauckner J, Frey P, Geula C. Comparative distribution of tau phosphorylated at Ser262 in pre-tangles and tangles. Neurobiol Aging 2003; 24: 767–76.

Lee VM, Balin BJ, Otvos L Jr, Trojanowski JQ. A68: a major subunit of paired helical filaments and derivatized forms of normal Tau. Science 1991; 251: 675–8.

Lee VM, Goedert M, Trojanowski JQ. Neurodegenerative tauopathies. Annu Rev Neurosci 2001; 24: 1121–59.

Liu F, Li B, Tung EJ, Grundke-Iqbal I, Iqbal K, Gong CX. Site-specific effects of tau phosphorylation on its microtubule assembly activity and self-aggregation. Eur J Neurosci 2007; 26: 3429–36.

Luna-Munoz J, Garcia-Sierra F, Falcon V, Menendez I, Chavez-Macias L, Mena R. Regional conformational change involving phosphorylation of tau protein at the Thr231, precedes the structural change detected by Alz-50 antibody in Alzheimer's disease. J Alzheimers Dis 2005; 8: 29–41.

Matsuo ES, Shin RW, Billingsley ML, Van deVoorde A, O'Connor M, Trojanowski JQ, et al. Biopsy-derived adult human brain tau is phosphorylated at many of the same sites as Alzheimer's disease paired helical filament tau. Neuron 1994; 13: 989–1002.

Mena R, Wischik CM, Novak M, Milstein C, Cuello AC. A progressive deposition of paired helical filaments (PHF) in the brain characterizes the evolution of dementia in Alzheimer's disease. An immunocytochemical study with a monoclonal antibody against the PHF core. J Neuropathol Exp Neurol 1991; 50: 474–90.

Mercken M, Vandermeeren M, Lubke U, Six J, Boons J, Van de Voorde A, et al. Monoclonal antibodies with selective specificity for Alzheimer Tau are directed against phosphatase-sensitive epitopes. Acta Neuropathol 1992; 84: 265–72.

Miki Y, Mori F, Tanji K, Kakita A, Takahashi H, Wakabayashi K. Accumulation of histone deacetylase 6, an aggresome-related protein, is specific to Lewy bodies and glial inclusions. Neuropathology 2011. Epub ahead of print.

Min SW, Cho SH, Zhou Y, Schroeder S, Haroutunian V, Seeley WW, et al. Acetylation of tau inhibits its degradation and contributes to tauopathy. Neuron 2010; 67: 953–66.

Mondragon-Rodriguez S, Basurto-Islas G, Santa-Maria I, Mena R, Binder LI, Avila J, et al. Cleavage and conformational changes of tau protein follow phosphorylation during Alzheimer's disease. Int J Exp Pathol 2008; 89: 81–90.

Mukaetova-Ladinska EB, Harrington CR, Roth M, Wischik CM. Biochemical and anatomical redistribution of tau protein in Alzheimer's disease. Am J Pathol 1993; 143: 565–78.

Novak M, Wischik CM, Edwards P, Pannell R, Milstein C. Characterisation of the first monoclonal antibody against the pronase resistant core of the Alzheimer PHF. Prog Clin Biol Res 1989; 317: 755–61.

Novak M, Jakes R, Edwards PC, Milstein C, Wischik CM. Difference between the tau protein of Alzheimer paired helical filament core and normal tau revealed by epitope analysis of monoclonal antibodies 423 and 7.51. Proc Natl Acad Sci U S A 1991; 88: 5837–41.

Novak M, Kabat J, Wischik CM. Molecular characterization of the minimal protease resistant tau unit of the Alzheimer's disease paired helical filament. EMBO J 1993; 12: 365–70.

Otvos L Jr, Feiner L, Lang E, Szendrei GI, Goedert M, Lee VM. Monoclonal antibody PHF-1 recognizes tau protein phosphorylated at serine residues 396 and 404. J Neurosci Res 1994; 39: 669–73.

Rankin CA, Sun Q, Gamblin TC. Tau phosphorylation by GSK-3beta promotes tangle-like filament morphology. Mol Neurodegener 2007; 2: 12.

Schmidt ML, Gur RE, Gur RC, Trojanowski JQ. Intraneuronal and extracellular neurofibrillary tangles exhibit mutually exclusive cytoskeletal antigens. Ann Neurol 1988; 23: 184–9.

Schneider A, Biernat J, von Bergen M, Mandelkow E, Mandelkow EM. Phosphorylation that detaches tau protein from microtubules (Ser262, Ser214) also protects it against aggregation into Alzheimer paired helical filaments. Biochemistry 1999; 38: 3549–58.

Schweers O, Schonbrunn-Hanebeck E, Marx A, Mandelkow E. Structural studies of tau protein and Alzheimer paired helical filaments show no evidence for beta-structure. J Biol Chem 1994; 269: 24290–7.

Seubert P, Mawal-Dewan M, Barbour R, Jakes R, Goedert M, Johnson GV, et al. Detection of phosphorylated Ser262 in fetal tau, adult tau, and paired helical filament tau. J Biol Chem 1995; 270: 18917–22.

Wischik CM, Novak M, Edwards PC, Klug A, Tichelaar W, Crowther RA. Structural characterization of the core of the paired helical filament of Alzheimer disease. Proc Natl Acad Sci U S A 1988; 85: 4884–8.

Wolozin BL, Pruchnicki A, Dickson DW, Davies P. A neuronal antigen in the brains of Alzheimer patients. Science 1986; 232: 648–50.

Xie SX, Baek Y, Grossman M, Arnold SE, Karlawish J, Siderowf A, et al. Building an integrated neurodegenerative disease database at an academic health center. Alzheimers Dement 2011; 7: e84–e93.

Yoshida M. Cellular tau pathology and immunohistochemical study of tau isoforms in sporadic tauopathies. Neuropathology 2006; 26: 457–70.